Rare Nuclearities and Unprecedented Structural Motifs in Manganese Cluster Chemistry from the Combined Use of Di-2-pyridyl Ketone with Selected Diols

Dedicated to Professor Spyros P. Perlepes, an excellent scientist, great teacher, valuable collaborator, and dear friend, on the occasion of his 70th birthday.

Katerina Skordi,[1] Dimitris I. Alexandropoulos,[1] Adeline D. Fournet,[2†] Nikos Panagiotou,[1] Eleni E. Moushi,[3] Constantina Papatriantafyllopoulou,[1‡] George Christou,[2] Anastasios J. Tasiopoulos[1,*]

[1] *Department of Chemistry, University of Cyprus, 1678 Nicosia, Cyprus.*
[2] *Department of Chemistry, University of Florida, Gainesville, Florida 32611, USA.*
[3] *Department of Life Sciences, School of Science, European University Cyprus, 1516 Nicosia, Cyprus*
[†] *Current address: Intel Corporation, Hillsboro, Oregon 97124, USA*
[‡] *Current address: School of Biological and Chemical Sciences, College of Science and Engineering, University of Galway, University Road, H91 TK33 Galway, Ireland.*
[*] Correspondence: atasio@ucy.ac.cy

Table S1. Crystal data and structural refinement parameters for compounds **1**·2DMF·H_2O, **2**, **3**·2MeCN, **4** and **5**·DMF.

Complex	**1**·2DMF·H_2O	**2**	**3**·2MeCN	**4**	**5**·DMF
Empirical formula	$C_{82}H_{97}N_{28}O_{38}Mn_{11}$	$C_{77}H_{85}N_{26}O_{35}Mn_{11}$	$C_{76}H_{90}Mn_{12}N_{16}O_{50}$	$C_{46}H_{54}N_8O_{18}Mn_4$	$C_{81}H_{77}N_{13}O_{29}ClMn_7$
Formula weight	2687.21	2538.04	2686.91	1226.73	2116.58
Temperature/K	101(2)	100(2)	100(2)	100(2)	100(2)
Crystal system	orthorhombic	orthorhombic	monoclinic	triclinic	monoclinic
Space group	Pbca	Pbca	C2/c	P-1	$P2_1/c$
a/Å	19.3661(5)	19.716(1)	34.543(3)	9.948 (1)	21.2869(6)
b/Å	32.8813(6)	32.7781(9)	20.816(2)	12.322(2)	20.0924(5)
c/Å	36.534(1)	36.607(2)	18.708(2)	12.792 (2)	24.9677(7)
α/°	90	90	90	106.386(8)	90
β/°	90	90	119.72(2)	102.623(8)	110.731(3)
γ/°	90	90	90	111.751(9)	90
Volume/$Å^3$	23264 (1)	23657 (2)	11683(2)	1302.2(2)	9987.4(5)
Z	8	8	4	1	4
$\rho_{calc}g/cm^3$	1.534	1.425	1.528	1.564	1.408
μ/mm^{-1}	10.125	1.211	1.339	8.403	0.961
F(000)	10912.0	10264.0	5432.0	630.0	4312.0
Crystal size/mm^3	0.09 × 0.046 × 0.014	0.09 × 0.046 × 0.014	0.09 × 0.046 × 0.014	0.09 × 0.046 × 0.014	0.09 × 0.046 × 0.014
Radiation	CuKα λ = 1.54184	MoKα λ = 0.71073	MoKα λ = 0.71073	CuKα λ = 1.54184	MoKα λ = 0.71073
2Θ range for data collection/°	6.652 to 133.996	6.164 to 50	5.86 to 50.144	7.73 to 133.994	6.426 to 50
Index ranges	-18 ≤ h ≤ 23 -33 ≤ k ≤ 39 -43 ≤ l ≤ 25	-23 ≤ h ≤ 22 -37 ≤ k ≤ 38 -43 ≤ l ≤ 31	-41 ≤ h ≤ 32 -24 ≤ k ≤ 17 -22 ≤ l ≤ 22	-10 ≤ h ≤ 11 -14 ≤ k ≤ 10 -15 ≤ l ≤ 14	-25 ≤ h ≤ 20 -23 ≤ k ≤ 23 -26 ≤ l ≤ 29
Reflections collected	52488	79820	24933	7512	48777
Independent reflections	20705 R_{int} = 0.0473 R_{sigma} = 0.0507	20629 R_{int} = 0.0909 R_{sigma} = 0.0978	10301 R_{int} = 0.0612 R_{sigma} = 0.0762	4615 R_{int} = 0.0421 R_{sigma} = 0.0626	17553 R_{int} = 0.0328 R_{sigma} = 0.0354
Data/restraints/ parameters	20705/16/1356	20629/82/1324	10301/129/732	4615/0/325	17553/81/1180
Goodness-of-fit on F^2	1.014	0.995	1.089	1.099	1.060
Final R indexes [I>=2σ (I)]	R_1[a] = 0.0805 wR_2[b] = 0.2363	R_1 = 0.0675 wR_2 = 0.1736	R_1 = 0.0604 wR_2 = 0.1638	R_1 = 0.0787 wR_2 = 0.2206	R_1 = 0.0777 wR_2 = 0.1902
Final R indexes [all data]	R_1 = 0.1029 wR_2 = 0.2561	R_1 = 0.1100 wR_2 = 0.1988	R_1 = 0.0814 wR_2 = 0.1793	R_1 = 0.0945 wR_2 = 0.2391	R_1 = 0.0858 wR_2 = 0.1946
Largest diff. peak/hole / e $Å^{-3}$	1.94/-1.24	1.19/-1.05	1.98/-1.19	1.19/-1.47	1.23/-1.21

[a] $R_1 = \Sigma(||F_o| - |F_c||)/\Sigma|F_o|$. [b] $wR_2 = [\Sigma[w(F_o^2 - F_c^2)^2]/\Sigma[w(F_o^2)^2]]^{1/2}$, $w = 1/[\sigma^2(F_o^2) + [(ap)^2 + bp]$, where $p = [\max(F_o^2, 0) + 2F_c^2]/3$.

Table S2. Bond valence sum (BVS)[c] calculations for Mn ions in **1-5.**

Complex **1**			
Atom	Mn(II)	Mn(III)	Mn(IV)
Mn1	1.82	1.70	1.72
Mn2	3.19	2.93	3.05
Mn3	3.09	2.86	2.95
Mn4	2.10	1.94	2.00
Mn5	2.03	1.87	1.94
Mn6	1.99	1.84	1.90
Mn7	1.94	1.79	1.85
Mn8	3.14	2.89	3.01
Mn9	3.26	3.04	3.10
Mn10	3.25	2.99	3.11
Mn11	1.86	1.74	1.76
Complex **2**			
Atom	Mn(II)	Mn(III)	Mn(IV)
Mn1	1.83	1.71	1.74
Mn2	3.25	2.98	3.11
Mn3	1.99	1.84	1.90
Mn4	3.12	2.89	2.97
Mn5	2.03	1.88	1.94
Mn6	2.01	1.86	1.92
Mn7	1.92	1.78	1.83
Mn8	3.16	2.91	3.02
Mn9	3.28	3.05	3.12
Mn10	3.20	2.96	3.08
Mn11	1.76	1.65	1.67
Complex **3**			
Atom	Mn(II)	Mn(III)	Mn(IV)
Mn1	1.88	1.73	1.79

Mn2	3.31	3.05	3.16
Mn3	1.92	1.78	1.84
Mn4	3.16	2.90	3.04
Mn5	3.19	2.94	3.05
Mn6	3.07	2.81	2.95

Complex **4**

Atom	Mn(II)	Mn(III)	Mn(IV)
Mn1	3.18	2.93	3.05
Mn2	1.91	1.76	1.83

Complex **5**

Atom	Mn(II)	Mn(III)	Mn(IV)
Mn1	3.30	3.05	3.15
Mn2	2.09	1.93	2.00
Mn3	3.26	3.00	3.12
Mn4	3.30	3.07	3.13
Mn5	3.28	3.02	3.14
Mn6	1.98	1.83	1.89
Mn7	3.26	3.02	3.12

[c] The underlined value is the one closest to the charge for which it was calculated. The oxidation state is the nearest whole number to the underlined value.

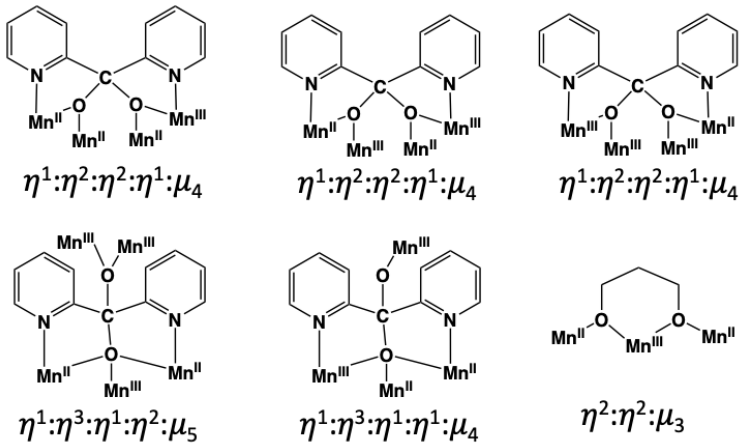

Scheme S1. Schematic representation of the coordination modes of $(py)_2CO_2^{2-}$ and pd^{2-} ligands in complex **1**.

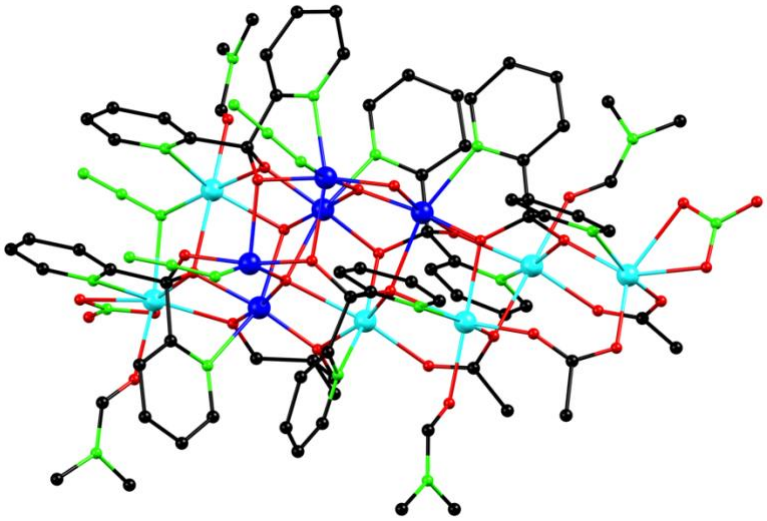

Figure S1. Ball and stick representation of the complete structure of **2**. H atoms are omitted for clarity. Colour code: Mn^{II}, cyan; Mn^{III}, blue; N, green; O, red; C, black.

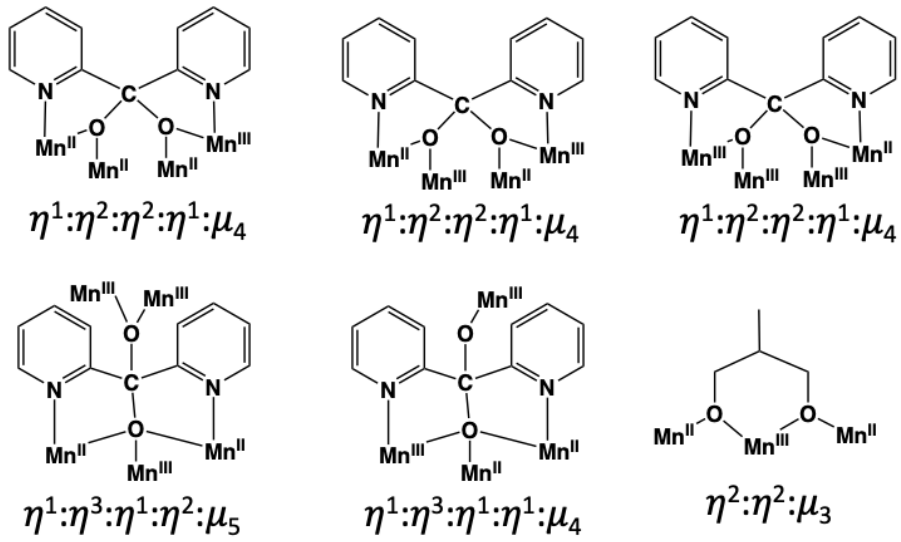

Scheme S2. Schematic representation of the coordination modes of $(py)_2CO_2^{2-}$ and pd^{2-} ligands in complex **2**.

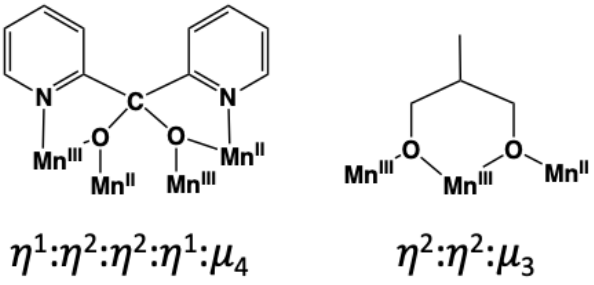

Scheme S3. Schematic representation of the coordination modes of $(py)_2CO_2^{2-}$ and mpd^{2-} ligands in complex **3**.

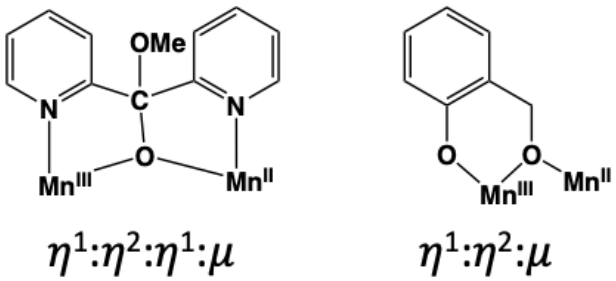

Scheme S4. Schematic representation of the coordination modes of $(py)_2C(OMe)O^-$ and $2\text{-}hp^{2-}$ ligands in complex **4**.

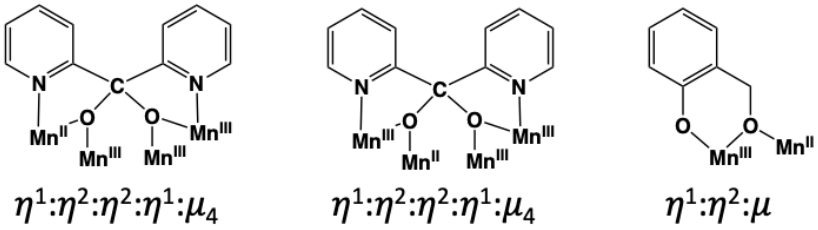

Scheme S5. Schematic representation of the coordination modes of $(py)_2CO_2^{2-}$ and $2\text{-}hp^{2-}$ ligands in complex **5**.

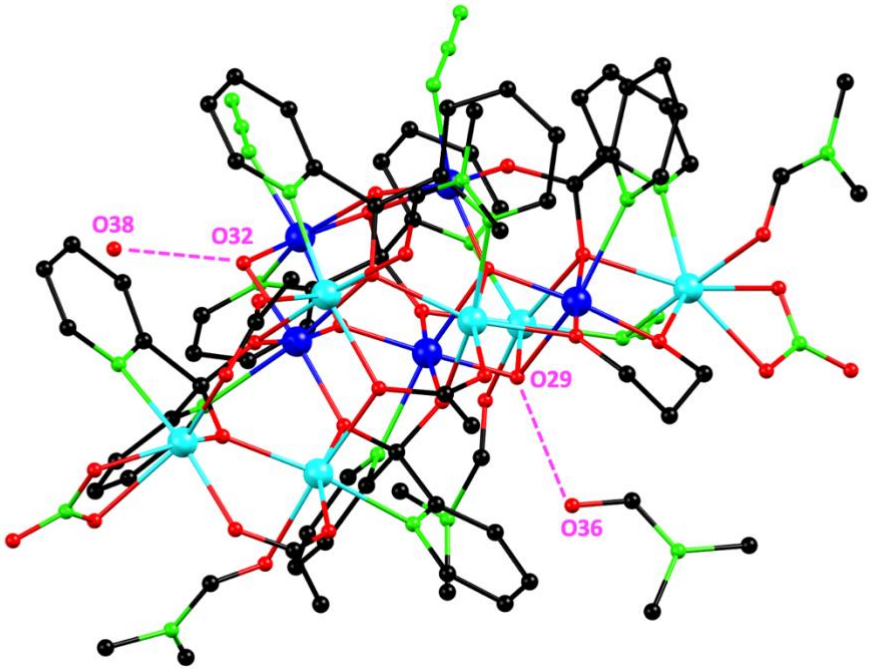

Figure S2. Hydrogen bonding in **1**, including interactions of a lattice H_2O (O38) molecule with a bridging OH^- (O32) anion (O38···O32 = 2.672(2) Å) and an O atom of a lattice DMF molecule (O36) with a bridging OH^- (O29) anion (O36···O29 = 2.756(4) Å). Colour code: Mn^{II}, cyan; Mn^{III}, blue; N, green; O, red; C, black. H atoms are omitted for clarity.

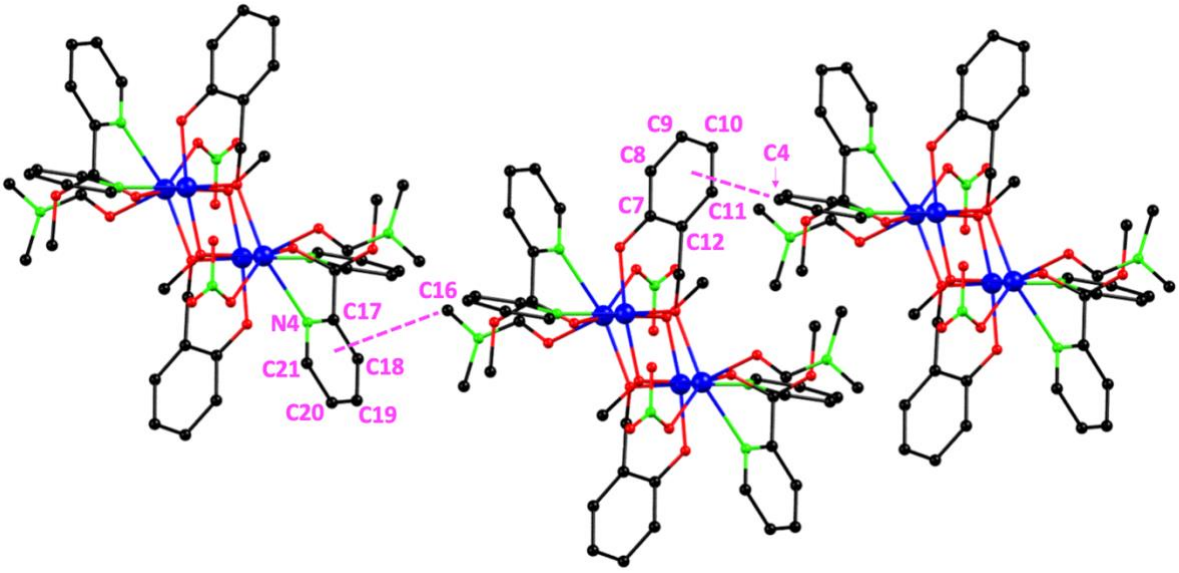

Figure S3. Intermolecular CH_3-π interactions between a coordinated DMF (C16) molecule with a pyridyl ring (C17C18C19C20C21N4) of the $(py)_2C(OMe)O^-$ ligand (C16…C17C18C19C20C21N4 = 3.677(9) Å), and T-shaped π-π stacking between a pyridyl ring (C4) of $(py)_2C(OMe)O^-$ ligand and a phenolic ring (C7C8C9C10C11C12) of 2-hp^{2-} anion (C4…C7C8C9C10C11C12 = 3.555(9) Å) in **4**. Colour code: Mn^{II}, cyan; Mn^{III}, blue; N, green; O, red; C, black. H atoms are omitted for clarity.

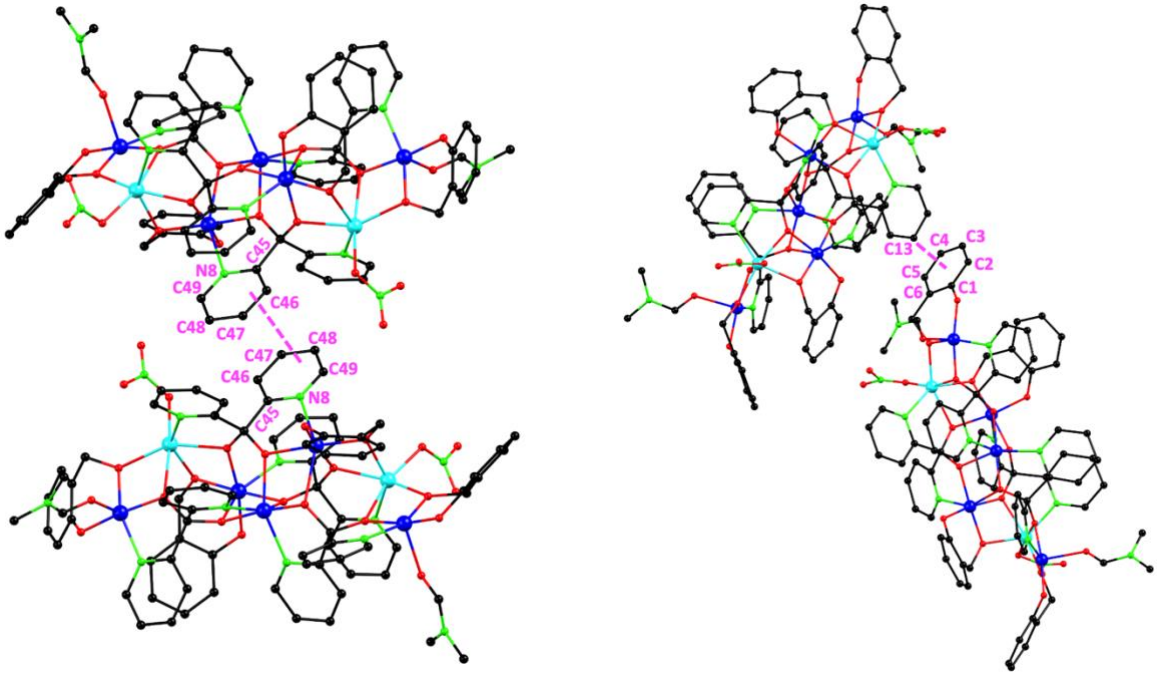

Figure S4. Intermolecular π-π stacking in **5**, including interactions (left) of the pyridyl rings (C45C46C47C48C49N8) of $(py)_2CO_2^{2-}$ anions (C45C46C47C48C49N8… C45C46C47C48C49N8 = 3.745(9) Å), and (right) of a pyridyl ring (C13) of $(py)_2CO_2^{2-}$ and a phenolic ring (C1C2C3C4C5C6) of 2-hp^{2-} anions (C13…C1C2C3C4C5C6 = 3.868(9) Å) of two adjacent cations of **5**. Colour code: Mn^{II}, cyan; Mn^{III}, blue; N, green; O, red; C, black. H atoms are omitted for clarity.

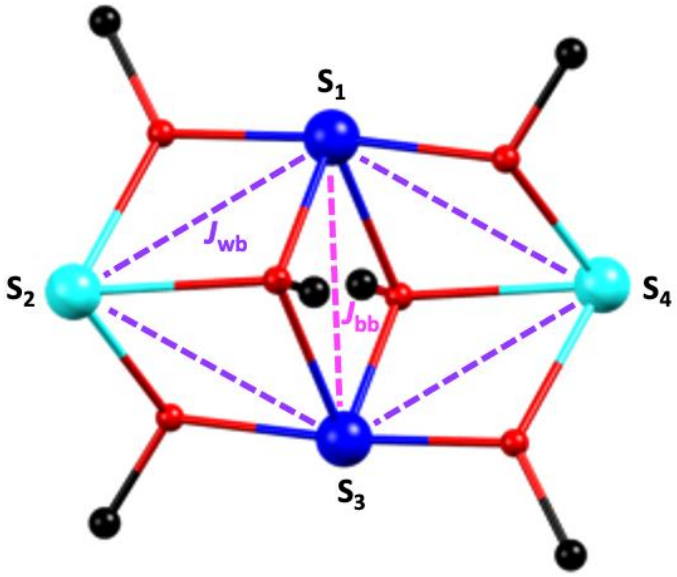

Figure S5. *J*-coupling scheme employed for the elucidation of magnetic exchange interactions in **4**.

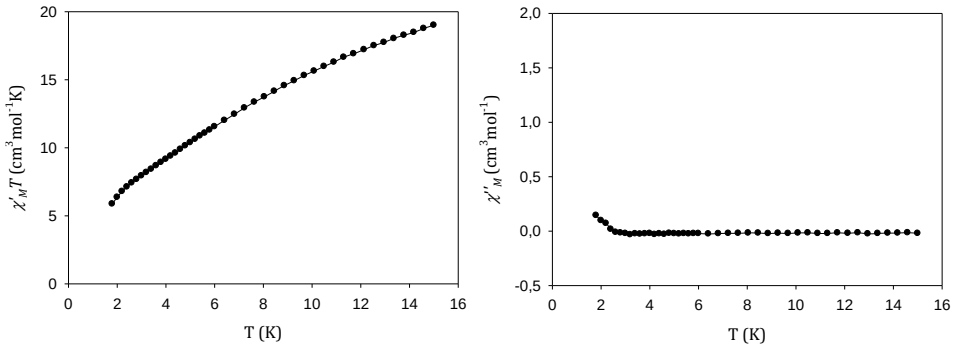

Figure S6. Temperature dependence of the in-phase $\chi'_M T$ product (left) and out-of-phase χ''_M (right) ac susceptibility signal of **3** in a 3.5 G field oscillating at 1000 Hz frequency.

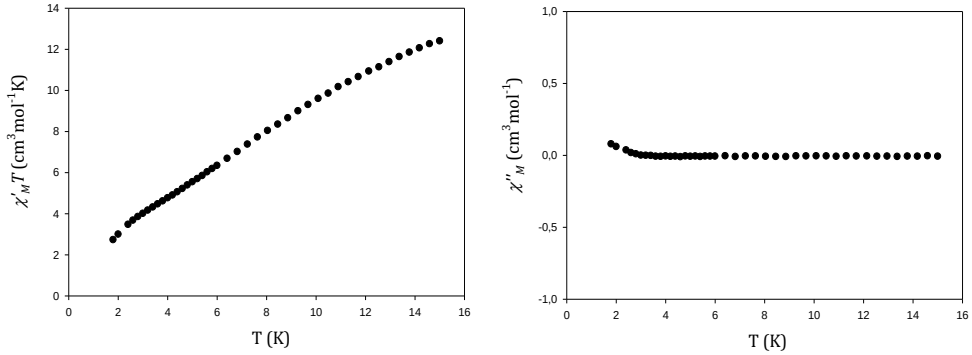

Figure S7. Temperature dependence of the in-phase $\chi'_M T$ product (left) and out-of-phase χ''_M (right) ac susceptibility signal of **4** in a 3.5 G field oscillating at 1000 Hz frequency.

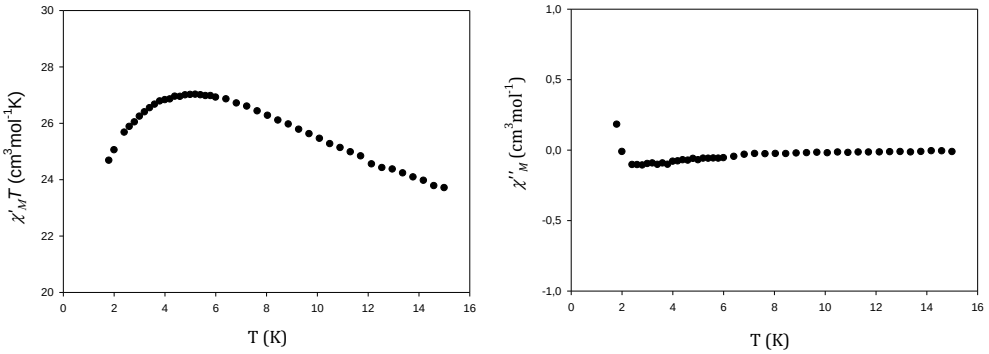

Figure S8. Temperature dependence of the in-phase $\chi'_M T$ product (left) and out-of-phase χ''_M (right) ac susceptibility signal of **5** in a 3.5 G field oscillating at 1000 Hz frequency.